41Ca in Tooth Enamel. Part II: A Means for Retrospective Biological Neutron Dosimetry in Atomic Bomb Survivors

Authors: Rühm, W., Wallner, A., Cullings, H., Egbert, S. D., El-Faramawy, N., et al.

---

[41]Ca in Tooth Enamel. Part II: A Means for Retrospective Biological Neutron Dosimetry in Atomic Bomb Survivors

W. Rühm,[a,b,1] A. Wallner,[b,c,d] H. Cullings,[e] S. D. Egbert,[f] N. El-Faramawy,[a,g] T. Faestermann,[c] D. Kaul,[f] K. Knie,[c]
G. Korschinek,[c] N. Nakamura,[e] J. Roberts[f] and G. Rugel[c]

[a] *Helmholtz Zentrum München, German Research Center for Environmental Health, 85764 Neuherberg, Germany;* [b] *Radiobiological Institute,
University of Munich, 80336 Munich, Germany;* [c] *Faculty of Physics, Technical University of Munich, 85747 Garching, Germany;*
[d] *VERA laboratory, Faculty of Physics, University of Vienna, A-1090 Wien, Austria;* [e] *Radiation Effects Research Foundation, Hiroshima, Japan;*
[f] *Science Applications International Corporation, San Diego, California 92121; and* [g] *On leave from Department of Physics, Faculty of Science,
Ain Shams University, 65511 Abbassia, Cairo, Egypt*

Rühm, W., Wallner, A., Cullings, H., Egbert, S. D., El-Faramawy, N., Faestermann, T., Kaul, D., Knie, K., Korschinek, G., Nakamura, N., Roberts, J. and Rugel, G. [41]Ca in Tooth Enamel. Part II: A Means for Retrospective Biological Neutron Dosimetry in Atomic Bomb Survivors. *Radiat. Res.* 174, 146–154 (2010).

[41]Ca is produced mainly by absorption of low-energy neutrons on stable [40]Ca. We used accelerator mass spectrometry (AMS) to measure [41]Ca in enamel of 16 teeth from 13 atomic bomb survivors who were exposed to the bomb within 1.2 km from the hypocenter in Hiroshima. In our accompanying paper (Wallner *et al.*, *Radiat. Res.* 174, 000–000, 2010), we reported that the background-corrected [41]Ca/Ca ratio decreased from 19.5×10^{-15} to 2.8×10^{-15} with increasing distance from the hypocenter. Here we show that the measured ratios are in good correlation with γ-ray doses assessed by electron paramagnetic resonance (EPR) in the same enamel samples, and agree well with calculated ratios based on either the current Dosimetry System 2002 (DS02) or more customized dose estimates where the regression slope as obtained from an errors-in-variables linear model was about 0.85. The calculated DS02 neutron dose to the survivors was about 10 to 80 mGy. The low-energy neutrons responsible for [41]Ca activation contributed variably to the total neutron dose depending on the shielding conditions. Namely, the contribution was smaller (10%) when shielding conditions were lighter (e.g., outside far away from a single house) and was larger (26%) when they were heavier (e.g., in or close to several houses) because of local moderation of neutrons by shielding materials. We conclude that AMS is useful for verifying calculated neutron doses under mixed exposure conditions with γ rays. © 2010 by Radiation Research Society

[1] Address for correspondence: German Research Center for Environmental Health, Institute of Radiation Protection, Ingolstädter Landstr. 1, 85764 Neuherberg, Germany; e-mail: Werner. ruehm@helmholtz-muenchen.de.

INTRODUCTION

Neutrons represent a densely ionizing radiation that is more effective biologically than X or γ rays. There are many occasions where neutrons contribute significantly to the dose of individuals or groups of individuals. For example, they are produced continuously in the atmosphere by cosmic radiation and contribute about half of the effective dose at flight altitudes (*1*). Occupational exposure to neutrons may occur in nuclear installations or outside the shielding of high-energy accelerators (*2*), and accidental exposures to large doses of neutrons have been reported (*3*). Fairly substantial exposures have also been reported as a by-product of proton therapy (*4*). Exposures to mixed radiation fields including neutrons occurred in the atomic bomb survivors of Hiroshima and Nagasaki (*5*). Retrospective dose estimation for these exposed individuals is always a difficult task.

In the past, the obvious need to quantify individual exposures to ionizing radiation retrospectively led to efforts aimed at finding traces of radiation exposure in biological materials of those exposed. Biological dosimetry—as it is called—primarily includes two methods; one is detection of chromosome aberrations (dicentric chromosomes shortly after exposure or translocations years after exposure) in peripheral blood lymphocytes, and the other is measurement of carbon radicals in tooth enamel by means of electron paramagnetic resonance (EPR). Translocation frequencies have been measured in a large number of atomic bomb survivors and carbon radicals in tooth enamel from several tens of survivors to substantiate or better understand possible biases in individual doses estimated physically (*6, 7*). However, no method is available to evaluate neutron exposures separately under mixed exposures, which include γ rays.

Despite those difficulties, efforts have been made over several decades to quantify the radiation doses to the survivors given the importance of the atomic bomb survivor cohort in radiation sciences; atomic bomb

146

survivor data that accumulated from 1950 up until recent years are being used as a basis for setting radiation safety standards world-wide (*8*). Regarding the assessment of neutron doses, a number of different neutron-induced radioisotopes have been quantified in environmental samples from Hiroshima and Nagasaki to reconstruct the neutron fluence at their locations (*5, 9–16*), while no appropriate methods are available for individual biological samples [see ref. (*17*) for more information]. In the present study, we propose a new method to estimate individual doses of neutrons using human teeth.

The proposed method includes measurements of the [41]Ca/Ca ratio in tooth enamel. [41]Ca ($t_{1/2} = 103,000$ years) is produced mainly by absorption of low-energy neutrons on stable [40]Ca. In a companion paper (*18*), we describe the methods used to prepare enamel samples and to detect the number of [41]Ca nuclei by means of accelerator mass spectrometry (AMS), and we apply it for the first time to enamel samples from atomic bomb survivors. In the present paper, we compare the measured [41]Ca/Ca ratios with the γ-ray dose measured by EPR and with calculated [41]Ca/Ca ratios based on the DS02 dosimetry system and on more customized simulations.

MATERIALS AND METHODS

Method of Detection

We propose detecting the long-lived radionuclide [41]Ca in tooth enamel in a manner similar to what we have reported previously for environmental granite samples (*19, 20*). In the samples, [41]Ca is produced by absorption of thermal neutrons on stable [40]Ca. Thus the [41]Ca/Ca ratio in an enamel sample is a direct measure of the neutron fluence to which the sample was exposed. Because the [41]Ca activity in a 100-mg enamel sample, which is typically available from individual molars, is far too low to detect by decay counting (e.g., the activity is less than 1 μBq), AMS is proposed for the measurement of [41]Ca, which identifies [41]Ca by its mass and nuclear charge prior to its decay. That technique allows detection of [41]Ca/Ca levels below 1×10^{-15} (which would correspond to about 0.1 μBq of [41]Ca activity in a 100-mg enamel sample). Details of the method are given in the companion paper (*18*).

Samples Investigated

Tooth enamel is considered the most suitable human biomaterial for [41]Ca detection because of its high calcium concentration, little if any metabolism after completion of tooth formation, and applicability of EPR for the assessment of γ-ray doses in the same sample (*7*). For the present study, 16 tooth enamel samples from 13 donors were chosen, which satisfied the following conditions: (1) he or she was exposed to the bomb between 0.8 km and 1.2 km from the hypocenter in Hiroshima; the hypocenter is the vertical projection to the ground of the point of explosion (i.e., the epicenter) that was 600 m above the ground (*5*); (2) a tooth sample was extracted for medical reasons and donated to the Radiation Effects Research Foundation (RERF); and (3) EPR measurements had already been performed on the samples to quantify the dose of γ rays from the bomb (*7*). Typically, 100 mg of enamel was available from each tooth, which corresponded to about 36 mg of calcium. Teeth from a control group with low exposure were also included in the study. See ref. (*21*) for more details.

Simulation of the [41]Ca/Ca Ratios in Individual Survivors Based on DS02

In an effort to calculate the [41]Ca/Ca ratio expected in tooth enamel of atomic bomb survivors, DS02 (*5*) was used as a reference. Among the organs considered in DS02, the thyroid gland was chosen as a surrogate because its mean depth below the skin is similar to that of the teeth in the oral cavity. Specifically, the [41]Ca/Ca ratio in the enamel samples was calculated for 10 investigated donors by multiplying the DS02 neutron fluence spectrum in the thyroid with the energy differential [40]Ca absorption cross-section (*22*) to calculate neutron-induced [41]Ca. DS02 house shielding, body size and individual orientation with respect to the direction to the epicenter were also taken into account as well as different possible postures (standing, sitting/kneeling, or lying). There is approximately a 20% systematic and 20% random uncertainty on the calculations. That based on the assumption that the uncertainty for total and thermal neutron fluence is similar to that of neutron dose (*23*). Figure 1 shows, as an example, the neutron fluence spectra as provided by DS02 at a distance where survivor D20 was located at the time of bombing. The fluence in each energy group is divided by the logarithmic width between the group's lower and upper energy bounds and then is normalized to the value for the thermal energy group. This presentation makes equal areas below the curve correspond to equal neutron fluence and allows each spectrum to be represented over a more narrow range for all energies to highlight differences among spectra. Because survivor D20 was exposed almost free-in-air, the DS02 neutron spectrum at that distance calculated free-in-air and 1 m above ground (i.e., without any disturbing building structures; light gray line in Fig. 1) is not much changed when DS02 standard procedures were included to take surrounding shielding structures into account (dark gray line in Fig. 1). The DS02 neutron spectrum in the thyroid, however, becomes more thermalized (black line in Fig. 1) due to moderation of neutrons in the human body. For comparison, Fig. 2 shows neutron fluence spectra for survivor E90, who was also exposed in the open but very close to adjacent buildings. In this case, the DS02 neutron spectrum that takes shielding into account (dark gray line in Fig. 2) differs much from the DS02 free-in-air spectrum at that distance (light gray line in Fig. 2) and is much softer. For the thyroid, the DS02 neutron spectrum (black line in Fig. 2) is still softer. Here, compared to survivor D20, the relative contribution of neutrons above say 100 keV, which are important for neutron dose, is reduced, and the role of thermal neutrons in dose becomes more important (see discussion below). Note also that the DS02 free-in-air spectrum for survivor D20 appears to be somewhat harder due to the hardening of the neutron spectrum with increasing distance from the hypocenter [corrected ground ranges are 1,057 m for D20 and 894 m for E90, respectively (Table 1)]. Given these neutron fluence spectra and the [41]Ca production cross-section, most of the [41]Ca nuclei produced in the enamel samples were due to neutrons below 0.4 eV (first bin in Figs. 1 and 2) (*18*).

DS02 does not calculate each individual's unique shielding situation directly but translates the individual's shielding parameters to a limited number of model shielding cases. Therefore, in an effort to improve the DS02 procedure, customized shielding calculations for the donors in this study were performed (*23*) by means of the MASH code (*24*). For that, the shielding history of each survivor had to be modeled individually. To achieve that, we used questionnaire information, which was collected in the early phase of the life span study (LSS) project in the 1950s. It contained locations of survivors at the time of the bombing with respect to the hypocenter, detailed shielding conditions by houses or other neighborhood structures, and orientation of the survivor with respect to the epicenter, posture, etc. The summary information is given in Table 1. Figure 3 gives, as an example, the environment where the individual who donated sample D20 survived (as modeled in the present paper for the customized approach). For comparison, Fig. 4 shows the donor of the E90 sample, who was exposed to radiation close to a cluster of Japanese
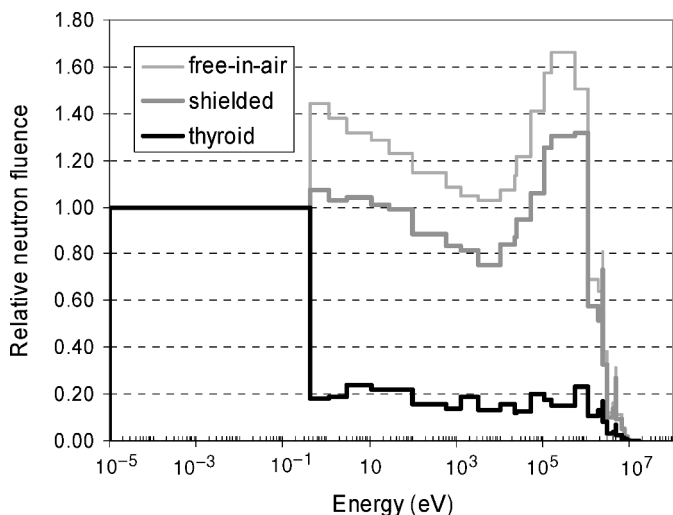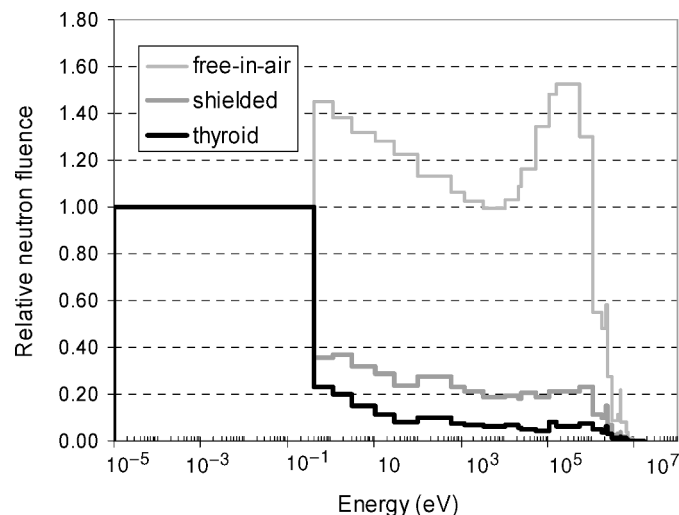
FIG. 1. Neutron fluence spectra for survivor D20 (DS02 ground range: 1,053 m) as provided by DS02. Light gray line: free-in-air 1 m above ground; dark gray line: including surrounding structures; black line: within thyroid.

FIG. 2. Neutron fluence spectra for survivor E90 (DS02 ground range: 893 m) as provided by DS02. Light gray line: free-in-air 1 m above ground; dark gray line: including surrounding structures; black line: within thyroid.

houses, with complicated conditions that require detailed modeling. With that customized approach, neutron energy spectra were calculated for the position of the survivor at the time of the bombing.

The customized approach calculated the individual neutron energy spectra at the survivors' in-house locations but did not include calculations of neutron energy spectra within the survivors' bodies. Therefore, to obtain a customized ^{41}Ca activation at the position of the thyroid gland of the donors, the standard DS02 total neutron fluences in the house (corresponding to the dark gray lines in Figs. 1 and 2) were adjusted to equal the total neutron fluence in the house obtained by the customized MASH calculations, and the resulting adjustment factor was used to renormalize the DS02 neutron energy spectrum in the thyroid gland. This is because ^{41}Ca activation in the thyroid gland is closely related to the total neutron fluence impinging on the body (for the adjustment factor, see column 6 of Table 1). In contrast to those survivors who provided samples I29, B51/53 and L80 and who received adjustment factors of 1.27, 1.27 and 1.23, respectively, the survivor who provided sample C47 also survived in a school building but received a much lower adjustment factor of 0.68. That difference is due to the fact that the former survivors' school building had a side with an unshielded exposure to the bomb, while the latter survivor had a two-story wing of the building, 12 m in front, near the line of sight, that blocked half of the incident neutron fluence. Neither large open classrooms nor building wings were included in the DS02 neutron calculations for Japanese wooden houses. The customized thyroid neutron fluence was multiplied by the ^{40}Ca neutron absorption cross section (22) to customize the ^{41}Ca production in the thyroid.

Re-evaluation of DS02 Ground Ranges by Means of Aerial Photographs

Values for the ground ranges of the survivors studied were initially taken from the DS02 database, and the customized shielding calculations described above were performed based on these values. The values are based on coordinates that were assigned to survivors in the 1950s and early 1960s, when survivors' shielding histories were created, using the plane rectangular coordinate system of the U.S. Army maps of 1945. Recently, in a further customized approach to improve the individual information available for the investigated survivors, the ground range values were re-evaluated based on prebombing aerial photographs showing detailed street plans and individual neighborhood houses, and survivors were located in

relation to the estimated locations of the hypocenters using a geographical information system (GIS) and a set of newer and more accurate maps (25). From a fit of the DS02 ground ranges as a function of total neutron fluence free-in-air ($\phi_{tot,fia,DS02gr}$), adjustments in the total neutron fluence due to the re-evaluation of the ground ranges were calculated for each survivor. It was assumed that a change in ground range would affect the total neutron fluence but would not change the neutron energy spectrum appreciably over the distances corresponding to the differences between each survivor's ground range in the RERF database and the more accurate ground range determined with aerial photographs, which were all <40 m. Therefore, the customized neutron spectra were corrected by multiplying by the $\phi_{tot,fia,corrected-gr}/\phi_{tot,fia,DS02-gr}$ ratio (column 5 in Table 1).

RESULTS AND DISCUSSION

For the samples investigated, we obtained gross ^{41}Ca/ Ca ratios varying from 4.0×10^{-15} to 23×10^{-15}. A background level of $(1.72 \pm 0.46) \times 10^{-15}$ was then subtracted, which was obtained from measurement of six control samples from distant survivors whose estimated γ-ray doses are below 0.5 mGy (18). The resulting net ^{41}Ca/Ca ratios ranged from 2.8×10^{-15} to 19.5×10^{-15} (Table 2). Because of the limited number of detected counts, statistical uncertainties dominate the overall uncertainties (13–24%). The results clearly demonstrate a systematic decrease of the ^{41}Ca/Ca ratios with increasing distance from the hypocenter, which suggests that A-bomb neutrons are the primary cause of the measured ^{41}Ca signal (18).

The measured ^{41}Ca/Ca ratios can be compared with the γ-ray doses measured by EPR on the same enamel samples (7). The results are also included in Table 2 and plotted in Fig. 5. A significant positive correlation is observed between the measured ^{41}Ca/Ca ratios and the γ-ray dose, which is expected because the distance from

TABLE 1
Basic Information on the Samples Used for the Present Study

Sample ID[a]	Age of donor at the time of bombing (years)	DS02 ground range (m)	Customized ground range (m)[b]	Correction factor for total free-in-air neutron fluence[c]	Correction factor for neutron fluence in customized house[d]	Type of shielding	Individual position	Individual shielding calculation
F04	19	827	827[f]	1.0[f]	-	–	–	no
H43	17	884	884[f]	1.0[f]	-	–	–	no
E90	14	893	894	0.98	0.89	Free-in-air (Fig. 4)	In front of and close to house cluster	yes
G91+G65	20	962	952	1.08	1.02	Twin house	First floor	yes
A72+A34	10	942	956	0.90	1.22	Triple house	First floor	yes
M93	17	1,000	1,000[f]	1.0[f]	0.93	House cluster	First floor	yes
K67	18	1,019	1,018	1.0	1.19	House cluster	First floor	yes
D20	14	1,053	1,057	0.97	0.97	Free-in-air (Fig. 3)	Far away from house	yes
I29[e]	19	1,148	1,108	1.34	1.27	School building	Second floor	yes
B51+B53[e]	18	1,148	1,111	1.31	1.27	School building	First floor	yes
L80[e]	18	1,153	1,116	1.32	1.23	School building	Second floor	yes
C47	33	1,132	1,124	1.05	0.68	School building	First floor	yes
J66	27	1,163	1,163[f]	1.0[f]	-	–	–	no

[a] Tooth samples G91 and G65, A72 and A34, and B51 and B53 are from the same survivor, respectively.
[b] DS02 ground ranges re-evaluated from aerial photographs when possible.
[c] Based on the re-evaluated ground ranges.
[d] I.e., the ratio of total customized MASH neutron fluence at the survivors' locations to the total DS02 neutron fluence at these locations.
[e] Survivors who donated the samples I29, B51 + B53 and L80 survived in the same school building.
[f] No aerial photograph available to correct for.

the hypocenter is the major parameter influencing both neutron and γ-ray doses of individual survivors in Hiroshima (but the neutron dose decreases faster than the γ-ray dose in the air with increasing distance from the hypocenter). In fact, based on DS02 free-in-air neutron and γ-ray energy spectra (26), the curvilinear dependence is expected to be similar to that observed in Fig. 5. It should be mentioned, however, that shielding of the survivors (for example by intervening building material) acts somewhat differently for neutrons and γ rays, which explains at least part of the scatter seen in Fig. 5.

Since the measured [41]Ca/Ca ratios indicate a close correlation with both the distance from the hypocenter
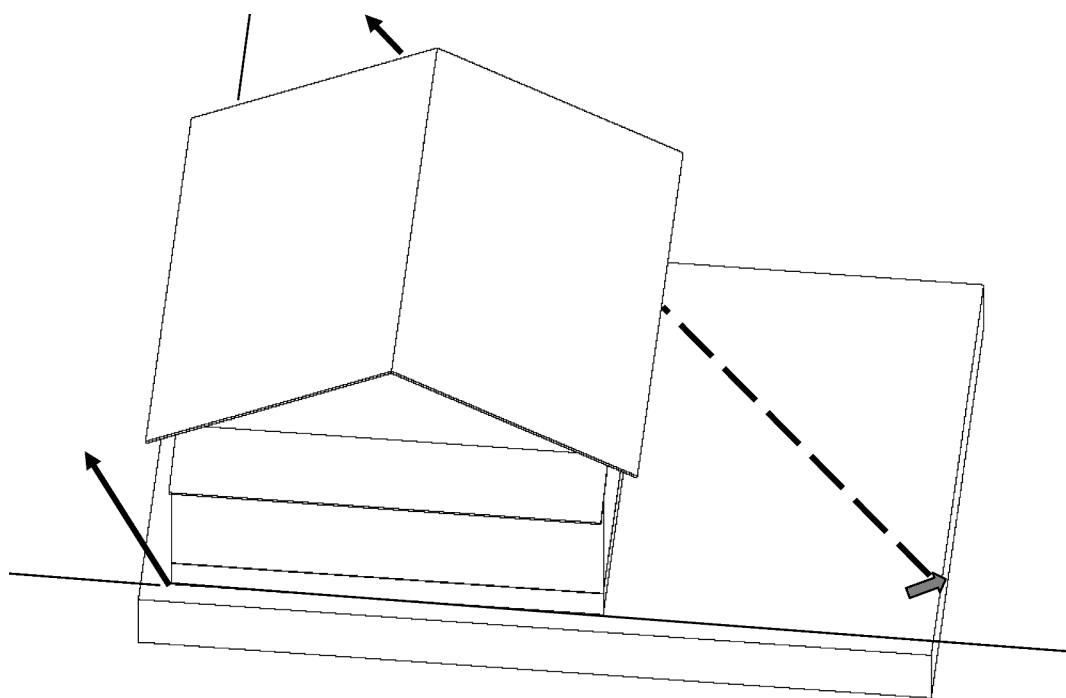
FIG. 3. Model of the environment in which the individual who donated sample D20 survived. Gray arrow: survivor location and orientation; solid black arrow: direction to epicenter from house origin; dashed black arrow: direction to hypocenter from survivor location.

RÜHM *ET AL.*
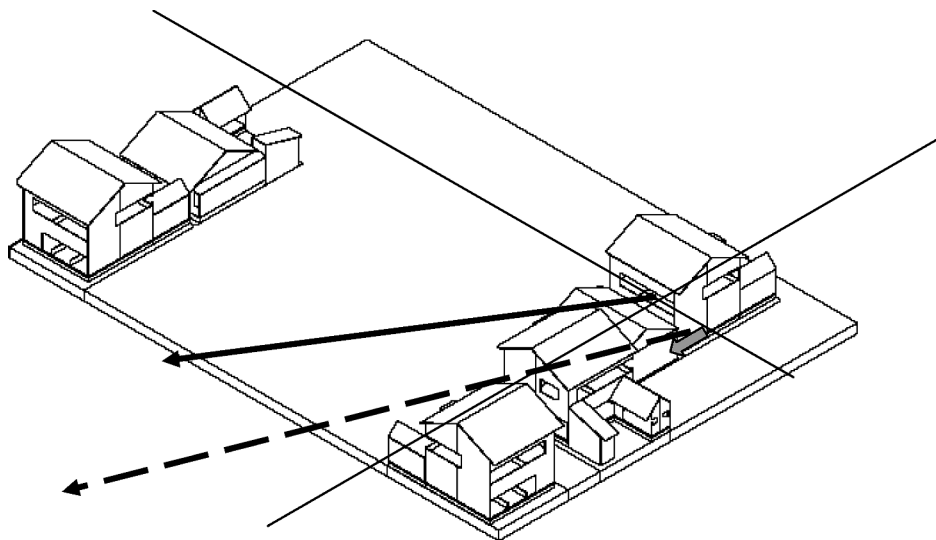
FIG. 4. Model of a house cluster where the individual who donated sample E90 survived. Gray arrow: survivor location and orientation; solid black arrow: direction to epicenter from house cluster origin; dashed black arrow: direction to hypocenter from survivor location.

(Table 1) (*18*) and the measured γ-ray dose (Fig. 5), ^{41}Ca in enamel can be considered as a biomarker for neutron exposure. To be a biodosimeter, however, the measured ^{41}Ca/Ca ratios need to be validated quantitatively. To address this issue, we calculated the ^{41}Ca/Ca ratio at the position of the thyroid for 10 donors by means of the MASH code, which used detailed shielding and incorporated the new information on ground ranges. The results of those calculations are also included in Table 2 and are compared with the measured ^{41}Ca/Ca ratios in Fig. 6. The measured ratios are generally proportionally

related to the calculated ones, but the mean slope was 0.68, which is somewhat lower than unity (Fig. 6). There may be several causes for this.

Based on the uncertainty discussion above, about 20% systematic and 20% random uncertainty may be involved in the ^{41}Ca activation calculations due to uncertainties, e.g., in survivor location and shielding conditions. Thus the total uncertainty in the calculated ^{41}Ca/Ca ratios may not be better than about 30%, which may explain part of the observed discrepancy. To be more specific, a slope of 0.68 was obtained by applying a

TABLE 2
**Results Obtained on the Investigated Tooth Enamel Samples**

Sample ID[a]	Tooth position[b]	EPR γ-ray dose (Gy)[c,d]	DS02 γ-ray dose for thyroid (Gy)	Net ^{41}Ca/Ca measured (10^{-15})[d]	^{41}Ca/Ca for thyroid based on customized calculation (10^{-15})	Total DS02 neutron dose for thyroid (mGy)
F04	7	3.1 ± 0.1	2.8	19.5 ± 4.0	-	82
H43	6	2.5 ± 0.1	2.7	13.5 ± 2.0	-	71
E90	1	2.3 ± 0.1	2.3	16.9 ± 4.1	23.6	50
G91	7	3.1 ± 0.1	2.5	11.3 ± 2.3	19.3	44
G65	6	2.7 ± 0.1	2.5	9.1 ± 2.0	19.3	44
A72	2	3.6 ± 0.1	2.8	18.2 ± 4.0	22.2	45
A34	3	3.9 ± 0.1	2.8	18.5 ± 4.0	22.2	45
M93	8	1.2 ± 0.1	2.1	7.2 ± 2.5	10.1	23
K67	6	1.2 ± 0.1	1.2	5.0 ± 1.5	14.4	29
D20	7	2.7 ± 0.1	2.8	8.6 ± 2.7	13.2	58
I29	8	1.8 ± 0.1	1.2	3.9 ± 2.0	8.7	15
B51	4	2.4 ± 0.1	1.1	7.4 ± 2.1	6.3	9.5
B53	4	2.4 ± 0.1	1.1	7.5 ± 2.4	6.3	9.5
L80	7/8	1.7 ± 0.1	1.0	7.6 ± 2.0	8.0	13
C47	8	2.8 ± 0.1	1.7	6.0 ± 2.1	2.4	13
J66	7	1.2 ± 0.1	0.8	2.8 ± 3.0	-	11

[a] Tooth samples G91 and G65, A72 and A34, and B51 and B53 are from the same survivors.
[b] Positions 1–2: incisor, position 3: canine, positions 4–5: premolar, positions 6–7: molar, position 8: wisdom tooth.
[c] Samples E90, A72, A34, B51 and B53, are non-molars, and the EPR γ-ray dose may include a contribution from exposure to ultraviolet light (*27*).
[d] Uncertainties refer to measurement errors including statistics and systematic 1 σ uncertainties (for details see text).
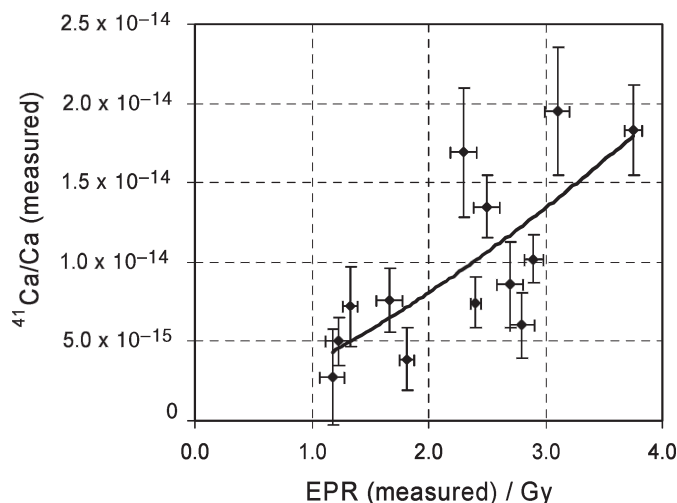
FIG. 5. Plots of [41]Ca/Ca ratios measured by AMS (*18*) as a function of γ-ray dose measured by EPR (*7*) in the same enamel samples. Data were fitted by a curvilinear non-weighted method (solid line); for multiple samples from the same survivors, weighted averages were used.

FIG. 6. Comparison of the measured and calculated [41]Ca/Ca ratios, which used detailed shielding information. The line shows a linear non-weighted fit of the data ($r^2 = 0.61$). Horizontal error bars are based on an assumed 30% uncertainty of the calculated [41]Ca/Ca ratios (see text for details).

regular regression model where the independent variables (the calculated [41]Ca/Ca ratios of the *x* axis) were assumed to be exact. However, the calculated [41]Ca/Ca ratios are subject to an error of about 30%, and an errors-in-variables model should therefore be applied instead, which would result in an attenuation of the slope as obtained from the regular regression model. If the error of the independent calculated variable corresponds roughly to 0.38×10^{-14} (which is 30% of the mean calculated value of 1.3×10^{-14}), then, given that the calculated values have a standard deviation of 0.72×10^{-14}, the expected attenuation in the regression slope is about $1/(1 + (0.38/0.72)^2) = 0.78$ [see e.g. ref. (*28*)]. A simulation of the data taking into account the Poisson counting statistics required due to the low number of counts measured confirmed this estimate and resulted in a value of 0.82 for the attenuated slope. The slope of about 0.68 obtained from the simple linear regressions is well within the 95% confidence bounds of the slopes obtained from the simulation, confirming that the results of the simple linear regressions do not statistically reject the null hypothesis that the measured and calculated values are estimating the same quantity. In summary, the estimated error of about 30% in the calculated values results in an attenuation of the slope obtained in the simple regression model of about 0.8. Correcting for this effect, the slope as obtained from Fig. 6 translates to $0.68/0.8 = 0.85$, which is still lower than but quite close to the ideal number of 1.

Additionally, some portion of the lower response could be due to the trend that, at high doses, those who actually survived were more likely to have received smaller true doses than their DS02 calculated dose, because those whose doses were higher (lower) than their DS02 doses were less likely (more likely) to have
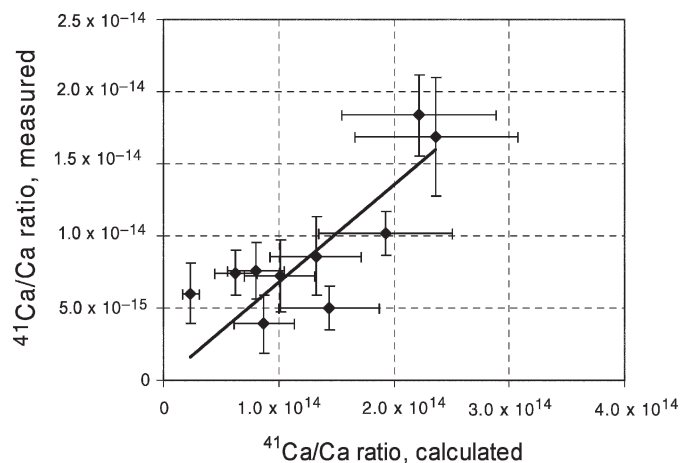
survived. However, this does not seem to be a likely explanation in the present study since the EPR-measured γ-ray doses are generally in good agreement with (or not smaller than) DS02-calculated γ-ray absorbed doses of the thyroid (Table 2). Note also that, due to their small number, the individuals studied may not be a representative sub-sample of the total LSS cohort. Finally, calcium isotope exchange processes between enamel and environment after the bombing could also explain a lower measured than calculated [41]Ca/Ca ratio, because natural [41]Ca/Ca ratios in the diet are low and of the order of 1×10^{-15} as indicated by the low ratios measured in the background enamel samples. Note, however, that the age of all survivors studied is such that enamel formation can be considered to have been completed at the time of bombing (see Table 1). We thus feel that the present results indicate that [41]Ca measurement is a useful biodosimeter of neutrons. Nevertheless, future investigations are needed to quantify, for example, any difference in [41]Ca activation in the thyroid compared to that in tooth enamel.

Figure 7 represents a comparison of the measured [41]Ca/Ca ratios with the ratios by standard DS02 calculations. Although the calculated ratios in some survivors may differ by about 40% between the standard DS02 and customized calculations, the mean slope (i.e., 0.69) remains nearly the same between Figs. 6 and 7 ($r^2 = 0.56$ for the DS02 approach and 0.61 for the customized calculations). Thus the results indicate that DS02 provides sufficient precision to quantify survivor exposure to neutrons. Although further calculations of detailed shielding and more accurate survivor locations are expected to improve the calculated ratios, the present results did not indicate the tendency clearly.

The last point relates to the detection limit of the AMS technique used to detect neutron exposures. Total
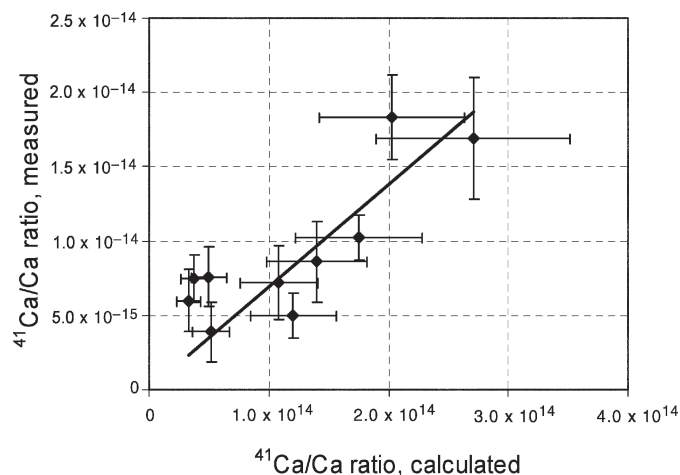
FIG. 7. Comparison of the measured and calculated ^{41}Ca/Ca ratios, which used standard DS02 calculations. The line shows a linear non-weighted fit of the data ($r^2 = 0.56$). Horizontal error bars are based on an assumed 30% uncertainty of the calculated ^{41}Ca/Ca ratios (see text for details).

FIG. 8. Fraction of DS02 absorbed dose to the thyroid from neutrons with energies below a specified energy relative to total neutron absorbed dose to the thyroid for two selected samples (D20 and E90).

neutron absorbed doses for the thyroids of the survivors examined were calculated based on the DS02 neutron spectra and were found to range from about 10 to 80 mGy (customized neutron spectra could not be calculated in the present study), which indicates that AMS is highly sensitive. Figure 8 shows the contribution of low-energy neutrons to the total neutron absorbed dose for the thyroid for the two survivors who donated samples D20 and E90. For the donor of the D20 sample, who was exposed in the open, the dose contribution of thermalized neutrons (<0.4 eV), which dominate ^{41}Ca production, was only about 10% to the total neutron dose. By contrast, for the donor of the E90 sample, who was exposed to the bomb very close to a cluster of Japanese houses, the contribution of thermalized neutrons was larger, about 26%. The difference is attributable to differences in the energy spectrum of the neutrons; namely, if the exposure occurred outside far away from a house, the fraction of thermal neutrons was smaller (e.g., donor of sample D20), while it was much larger if the exposure occurred inside or close to a house as a result of effective scattering and moderation of neutrons by building structures (e.g., donor of E90 sample) (see Figs. 1 and 2). Since both survivors were the same age, body size is probably not a major factor for the differences we observed. Further, orientation would not be a major factor either, because the donor of the D20 sample was oriented with his left side to the hypocenter while the donor of the E90 sample was oriented with his right side to the hypocenter, which should not make much difference for neutron absorbed dose of the thyroid. Thus, depending on the shape of the neutron spectrum at a survivor's location, thermal neutrons may contribute considerably to the total neutron dose, which is mainly due to protons emitted
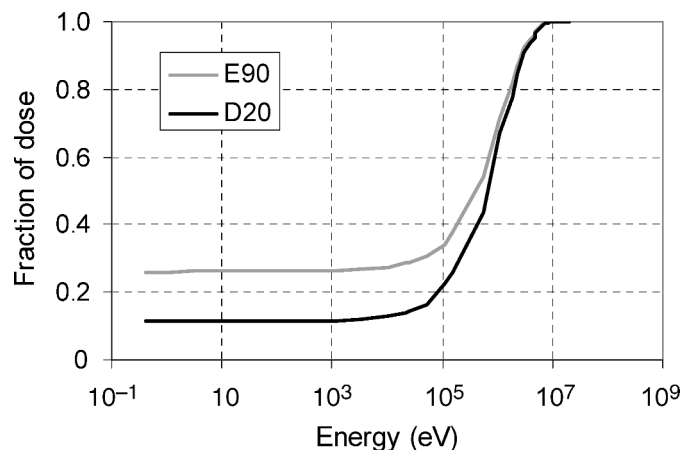
at an energy of about 0.6 MeV from ^{14}N($n_{thermal}$,p)^{14}C reactions that occur in tissue.

A contribution of thermal neutrons by 10–30% to the total neutron dose is similar to that of fast neutrons with an energy above 1 MeV (25–40%), which were considered to be the major contributor to the total neutron dose. For example, fast neutrons had been measured through the detection of ^{63}Ni in (inorganic) copper samples (*14, 15, 29, 30*) and through the detection of ^{39}Ar in (inorganic) granite samples (*16*). In these studies, samples that were exposed in the line of sight to the epicenter without much shielding were selected. Since the surrounding materials generally had a low moisture content, the neutron spectra were similar to those for survivors who were exposed in open conditions. Such survivors would have a smaller fraction of thermal neutrons compared with those who were more shielded or were surrounded by wooden structures at the time of the bombing. These studies showed that fast neutrons primarily contributed to the total neutron dose under circumstances of little shielding (e.g., survivors exposed in open conditions). By contrast, the present study showed that the contribution of thermal neutrons is also significant for those exposed in or close to a wooden house.

CONCLUSION

In summary, about 30 mg of the available 100 mg of tooth enamel was sufficient to measure both γ-ray doses by EPR and neutron exposure by ^{41}Ca AMS that were caused by atomic bomb radiation in 1945. Although the measured ^{41}Ca activation in enamel appears to be some 15% lower than that calculated, we feel that the present results indicate that ^{41}Ca measurement is a useful biodosimeter of neutrons. Nevertheless, additional work is required to quantify the origin of this remaining

discrepancy. That work may include, for example, detailed calculations to compare ^{41}Ca activation by neutrons in the thyroid (which was used as a proxy organ) compared to that in tooth enamel.

The present results are the first that document a biological fingerprint of neutron exposures in Hiroshima and Nagasaki, and ^{41}Ca AMS may detect neutron exposures that correspond to about 10 mGy of total neutron dose at a survivor's location in Hiroshima. The fact that the customized approach does not result in a substantial improvement over the standard DS02 approach suggests that the standard DS02 approach produces reliable individual dose estimates. This finding is important because it has not previously been verified experimentally for neutrons. The proposed method will serve as a unique tool for evaluating the neutron dose that accompanied γ-ray exposures. It may also be used to quantify accidental neutron exposures that occurred many years earlier.

REFERENCES

1. V. Mares, T. Maczka, G. Leuthold and W. Rühm, Air crew dosimetry with the new EPCARD.Net code. *Radiat. Prot. Dosimetry* **136**, 262–266 (2009).

2. B. Wiegel, S. Agosteo, R. Bedogni, M. Caresana, A. Esposito, G. Fehrenbacher, M. Ferrarini, E. Hohmann, C. Hranitzky and E. Weitzenegger, Intercomparison of radiation protection devices in a high-energy stray neutron field. Part II: Bonner sphere spectrometry. *Radiat. Meas.* **44**, 660–672 (2009).

3. M. S. Baxter, Ed., The Tokai-mura accident. *J. Environ. Radioact.* **50**, 1–172 (2000).

4. D. J. Brenner and E. J. Hall, Secondary neutrons in clinical proton radiotherapy: a charged issue. *Radiother. Oncol.* **86**, 165–170 (2008).

5. R. W. Young and G. D. Kerr, Eds., *Reassessment of the Atomic Bomb Radiation Dosimetry for Hiroshima and Nagasaki: Dosimetry System DS02*. Report of the Joint US-Japan Working Group. Radiation Effects Research Foundation, Hiroshima, 2005.

6. Y. Kodama, D. Pawel, N. Nakamura, D. Preston, T. Honda, M. Itoh, M. Nakano, K. Ohtaki, S. Funamoto and A. A. Awa, Stable chromosome aberrations in atomic bomb survivors: results from 25 years of investigation. *Radiat. Res.* **156**, 337–346 (2001).

7. N. Nakamura, C. Miyazawa, S. Sawada, M. Akiyama and A. A. Awa, A close correlation between electron spin resonance (ESR) dosimetry from tooth enamel and cytogenetic dosimetry from lymphocytes of Hiroshima atomic-bomb survivors. *Int. J. Radiat. Biol.* **73**, 619–627 (1998).

8. D. L. Preston, E. Ron, S. Tokuoka, S. Funamoto, N. Nishi, M. Soda, K. Mabuchi and K. Kodama, Solid cancer incidence in atomic bomb survivors: 1958–1998. *Radiat. Res.* **168**, 1–64 (2007).

9. B. Arakatsu, Report on survey of radioactivity in Hiroshima several days after the atomic bomb explosion. In *Collection of Investigative Reports on Atomic Bomb Disaster*, pp. 34–35. Science Council of Japan, Tokyo, 1953.

10. F. Yamasaki and A. Sugimoto, Radioactive ^{32}P in sulfur in Hiroshima. In *Collection of Investigative Reports on Atomic Bomb Disaster*, pp. 18–19. Science Council of Japan, Tokyo, 1953.

11. T. Hashizume, T. Maruyama, A. Shiragai, E. Tanaka, M. Izawa, S. Kawamura and S. Nagaoka, Estimation of the air dose from the atomic bombs in Hiroshima and Nagasaki. *Health Phys.* **13**, 149–161 (1967).

12. T. Nakanishi, T. Imura, K. Komura and M. Sakanoue, ^{152}Eu in samples exposed to the nuclear explosions at Hiroshima and Nagasaki. *Nature* **302**, 132–134 (1983).

13. G. Haberstock, J. Heinzl, G. Korschinek, H. Morinaga, E. Nolte, U. Ratzinger, K. Kato and M. Wolf, Accelerator mass spectrometry with fully stripped ^{36}Cl ions. *Radiocarbon* **28**, 204–210 (1986).

14. T. Straume, G. Rugel, A. A. Marchetti, W. Rühm, G. Korschinek, J. E. McAninch, K. Carroll, S. D. Egbert, T. Faestermann and C. Wallner, Measuring fast neutrons in Hiroshima at distances relevant to atomic-bomb survivors. *Nature* **424**, 539–542 (2003).

15. T. Straume, G. Rugel, A. A. Marchetti, W. Rühm, G. Korschinek, J. E. McAninch, K. Carroll, S. D. Egbert, T. Faestermann and H. Hasai, Addendum: Measuring fast neutrons in Hiroshima at distances relevant to atomic-bomb survivors. *Nature* **430**, 483 (2004).

16. E. Nolte, W. Rühm, H. H. Loosli, I. Tolstikhin, K. Kato, T. C. Huber and S. D. Egbert, Measurements of fast neutrons in Hiroshima by use of ^{39}Ar. *Radiat. Environ. Biophys.* **44**, 261–271 (2006).

17. W. Rühm, A. M. Kellerer, G. Korschinek, T. Faestermann, K. Knie, G. Rugel, K. Kato and E. Nolte, The dosimetry system DS86 and the neutron discrepancy in Hiroshima—historical review, present status, and future options. *Radiat. Environ. Biophys.* **37**, 293–310 (1998).

18. A. Wallner, W. Rühm, G. Rugel, N. Nakamura, A. Arazi, T. Faestermann, K. Knie, H. J. Maier and G. Korschinek, ^{41}Ca in tooth enamel. Part I: A biological signature of neutron exposure in atomic bomb survivors. *Radiat. Res.* **174**, 146–154 (2010).

19. G. Korschinek, H. Morinaga, E. Nolte, E. Preisenberger, U. Ratzinger, A. Urban, P. Dragovitsch and S. Vogt, Accelerator mass spectrometry with completely stripped ^{41}Ca and ^{53}Mn ions at the Munich tandem accelerator. *Nucl. Instrum. Methods B* **29**, 67–71 (1987).

20. W. Rühm, K. Kato, G. Korschinek, H. Morinaga and E. Nolte, ^{36}Cl and ^{41}Ca depth profiles in a Hiroshima granite stone and the Dosimetry System 1986. *Z. Phys. A* **341**, 235–238 (1992).

21. A. Wallner, A. Arazi, T. Faestermann, K. Knie, G. Korschinek, H. J. Maier, N. Nakamura, W. Rühm and G. Rugel, ^{41}Ca – a possible neutron specific biomarker in tooth enamel. *Nucl. Instrum. Methods B* **223–224**, 759–764 (2004).

22. M. B. Chadwick, P. Obložinský, M. Herman, N. M. Greene, R. D. McKnight, D. L. Smith, P. G. Young, R. E. MacFarlane, G. M. Hale and S. C. Frankle, Evaluated nuclear data file ENDF/B-VII. *Nucl. Data Sheets* **107**, 2931–3060 (2006).

23. D. C. Kaul, S. D. Egbert and W. A. Woolson, DS02 uncertainty analysis. In *Reassessment of the Atomic Bomb Radiation*

Dosimetry for Hiroshima and Nagasaki: Dosimetry System DS02 (R. W. Young and G. D. Kerr, Eds.), Vol. 2. Radiation Effects Research Foundation, Hiroshima, 2005.

24. J. O. Johnson, Ed., *A User's Manual for MASH v.2.0 – Monte Carlo Adjoint Shielding Code System*. Report ORNL/TM/11778/R2, Oak Ridge National Laboratory, Oak Ridge, TN, 1999.

25. H. M. Cullings, S. Fujita, M. Hoshi, S. D. Egbert and G. D. Kerr, Alignment and referencing of maps and aerial photographs. In *Reassessment of the Atomic Bomb Radiation Dosimetry for Hiroshima and Nagasaki: Dosimetry System DS02* (R. W. Young and G. D. Kerr, Eds.), Vol. 1, pp. 261–333. Radiation Effects Research Foundation, Hiroshima, 2005.

26. S. D. Egbert, G. D. Kerr and H. M. Cullings, DS02 fluence spectra for neutrons and gamma rays at Hiroshima and Nagasaki with fluence-to-kerma coefficients and transmission factors for sample measurements. *Radiat. Environ. Biophys.* **46**, 311–325 (2007).

27. N. El-Faramawy, Comparison of γ- and UV-light-induced EPR spectra of enamel from deciduous molar teeth. *Appl. Radiat. Isot.* **62**, 191–195 (2005).

28. N. R. Draper and H. Smith, *Applied Regression Analysis*, 2nd ed., pp. 122–125. Wiley, New York, 1981.

29. W. Rühm, K. L. Carroll, S. D. Egbert, T. Faestermann, K. Knie, G. Korschinek, R. E. Martinelli, A. A. Marchetti, J. E. McAninch and K. Shizuma, Neutron-induced ^{63}Ni in copper samples from Hiroshima and Nagasaki – a comprehensive presentation of results obtained at the Munich Maier-Leibnitz Laboratory. *Radiat. Environ. Biophys.* **46**, 327–338 (2007).

30. A. A. Marchetti, J. E. McAninch, G. Rugel, W. Rühm, G. Korschinek, R. E. Martinelli, T. Faestermann, K. Knie, S. D. Egbert and T. Straume, Fast neutrons measured in copper from the Hiroshima atomic bomb dome. *Radiat. Res.* **171**, 118–122 (2009).